A Phenomenological-Theoretical Proposal for a Non-Linear Vacuum Response to Intense Electromagnetic Fields in a Resonant Cavity

Martin Weysi

July 7, 2025

Abstract

This paper presents a phenomenological-theoretical framework to explore the hypothetical consequences of a non-linear, collective response of the quantum vacuum to intense, geometrically confined electromagnetic fields. We postulate that under specific resonant conditions, the vacuum may undergo a phase transition to a structured, metastable state. This possibility is formalized through an effective Lagrangian incorporating a complex scalar field, ψ, which is introduced as a phenomenological order parameter representing a coherent condensate of virtual electron-positron pairs. This framework is not derived from first principles but is presented as an exploratory tool. The dynamics of the ψ field and its gauge-invariant coupling to electromagnetism and gravity are derived from a unified action principle. We explicitly address the foundational challenges of this proposal, including the violation of Lorentz invariance and energy-momentum conservation, by grounding the framework in the energy supplied by the external stimulating field. A numerical simulation of a simplified 1D model is presented to demonstrate that the formation of localized, soliton-like structures is a natural outcome of the proposed non-linear dynamics. The paper concludes by exploring the phenomenological parameter space and calculating the physical conditions under which the gravitational effects of such a structured vacuum might become observable. This work is intended to stimulate future theoretical and experimental developments in the regime of strong-field QED.

1 Introduction

1.1 Context and Motivation: The Strong-Field QED Frontier

Quantum Electrodynamics (QED) has been tested to extraordinary precision in the perturbative regime [2]. However, the regime of extremely high field intensities, approaching the Schwinger limit $E_c \approx 1.3 \times 10^{18}\,\mathrm{V/m}$, remains a frontier of fundamental physics [12]. In this non-perturbative domain, the vacuum itself is expected to behave as a non-linear optical medium, an effect first described by the Euler-Heisenberg Lagrangian [21]. This

effective Lagrangian, derived by integrating out the one-loop effects of virtual electron-positron pairs, predicts phenomena like vacuum birefringence, revealing the vacuum as a dynamic, polarizable entity.

This paper explores a related, though more speculative, hypothesis: that an intense electromagnetic field, when confined within a resonant cavity, might induce not just a perturbative non-linear response, but a collective, non-linear phase transition of the vacuum state itself.

1.2 A Phenomenological-Theoretical Approach

A first-principles derivation of such a non-perturbative vacuum response from the fundamental QED Lagrangian is currently intractable. Therefore, we adopt a phenomenological approach, analogous to the Ginzburg–Landau theory of superconductivity. We introduce a complex scalar field, $\psi(x)$, as an effective order parameter to describe the state of the vacuum. This framework is not intended to be a fundamental derivation, but a phenomenological tool to stimulate future theoretical and experimental developments.

1.2.1 Microphysical Justification

We motivate the physical origin of ψ by proposing that it represents a coarse-grained, macroscopic field describing a coherent condensate of virtual electron-positron pairs. In the standard vacuum, these pairs fluctuate incoherently. Under a strong, resonant pumping field, we hypothesize that these pairs could form a coherent, Bose-like condensate. The amplitude $|\psi|$ would represent the density of this condensate.

2 A Proposed Lagrangian Framework

To ensure theoretical consistency, we build our framework upon a unified action principle.

2.1 The Effective Action

The total action for the system is postulated as:

$$S = \int d^4x \sqrt{-g} \left(\mathcal{L}_{GR} + \mathcal{L}_{EM} + \mathcal{L}_{\psi} \right)$$

Where:

- **Gravity** ($\mathcal{L}_{GR}$): The standard Einstein-Hilbert Lagrangian.
- **Electromagnetism** ($\mathcal{L}_{EM}$): The standard Lagrangian for the electromagnetic field.
- **Vacuum Order Parameter Field** ($\mathcal{L}_{\psi}$):

$$\mathcal{L}_{\psi} = g^{\mu\nu}(D_\mu\psi)^*(D_\nu\psi) - V(|\psi|^2) - \xi R|\psi|^2$$

Here:

- The gauge-invariant covariant derivative is:

$$D_\mu = \nabla_\mu - iqA_\mu \quad \text{with} \quad q = 2e$$

- The self-interaction potential is:

$$V(|\psi|^2) = -\mu^2|\psi|^2 + \lambda|\psi|^4$$

- The non-minimal coupling to curvature is:

$$\xi R|\psi|^2 \quad \text{with conformal coupling} \quad \xi = \frac{1}{6}$$

2.2 Derived Field Equations

Applying the principle of least action to the total action yields the full set of coupled, gauge-invariant field equations:

- Modified Einstein Field Equations (not explicitly shown here),
- Modified Maxwell's Equations with source terms from ψ,
- Nonlinear Klein–Gordon equation for ψ.

2.3 Limits of Applicability and Theoretical Considerations

Our model is formulated as an Effective Field Theory (EFT), aimed at describing novel phenomena beyond standard QED in the strong-field regime.

For context, we compare our model to two major EFT frameworks:

Euler–Heisenberg Effective Lagrangian:

$$\mathcal{L}_{EH} = \frac{1}{2}(E^2 - B^2) + \frac{2\alpha^2}{45m_e^4c^5\hbar^3}\left[(E^2 - B^2)^2 + 7(E \cdot B)^2\right]$$

This predicts vacuum birefringence but introduces no new dynamical fields or phase transitions.

Proposed Model: Introduces a complex scalar field ψ as a macroscopic order parameter. Allows:

- Spontaneous symmetry breaking,
- Soliton-like vacuum node formation,
- Gravitational and quantum optical signatures.

Comparison Table:

Ultraviolet Cutoff: As an EFT, the model is valid up to

$$\Lambda_{\text{UV}} \approx 2m_ec^2 \approx 1.022\,\text{MeV}$$

Beyond this, a UV-complete theory is needed.

Low-Field Limit: In the weak-field regime, the theory reduces exactly to

Feature	**Proposed Model**	**Euler–Heisenberg QED**	**Axion Electrodynamics**
New Degrees of Freedom	Complex scalar field ψ	None	Pseudoscalar axion field a
Lagrangian Structure	$\mathcal{L}_\psi = \lvert D_\mu\psi\rvert^2 - V(\psi)$	Non-linear corrections to $\mathcal{L}_{EM}$	$\mathcal{L}_{\text{axion}} = \frac{1}{2}(\partial_\mu a)^2 + ga\vec{E}\cdot\vec{B}$
Key Phenomenon	Vacuum phase transitions, soliton-like nodes	Vacuum birefringence, dichroism	Photon–axion conversions in magnetic fields
Symmetry Breaking	Spontaneous U(1) and translational symmetry	None	Peccei–Quinn (CP) symmetry
Experimental Signature	Gravitational waves, anomalous decays	Polarization rotation in strong fields	"Light shining through walls", haloscopes

Table 1: Comparison of features across three effective field theory frameworks.

Einstein-Maxwell theory. Standard photon-photon interactions remain governed by Euler–Heisenberg corrections. The postulation of the ψ field as a coherent condensate of virtual electron-positron pairs can be physically motivated by the Schwinger effect [12]. In the presence of an extremely strong electric field E, the quantum vacuum becomes unstable, leading to the spontaneous production of real e^-e^+ pairs. The rate of pair production per unit volume, Γ, is non-perturbative and given by:

$$\Gamma = \frac{(eE)^2}{4\pi^3 c\hbar^2}\sum_{n=1}^{\infty}\frac{1}{n^2}\exp\left(-\frac{n\pi m_e^2 c^3}{eE\hbar}\right)$$

For fields approaching the Schwinger limit $E_c \approx 1.3\times 10^{18}\,\mathrm{V/m}$, this rate becomes significant. As discussed by Di Piazza et al. [22], intense laser facilities are rapidly approaching the regime where this physics can be probed.

Our central hypothesis is that within a resonant cavity, this process can be stimulated and amplified. The cavity's resonant modes would preferentially select virtual pairs with specific momentum states, while the continuous pumping from the external laser field provides the energy to bring them to the mass shell. This resonant amplification could overcome the exponential suppression and drive a runaway process, leading to a high density of real pairs that subsequently cool and form a coherent, Bose-like condensate. The $\psi(x)$ field is introduced as the macroscopic order parameter describing this emergent state, where $|\psi|^2$ is proportional to the local density of the coherent pairs.

3 Dynamics and Stability of the Structured Vacuum

3.1 Numerical Simulation of Node Formation

To demonstrate that the proposed non-linear dynamics of the ψ field naturally lead to the formation of localized vacuum structures, we performed a numerical simulation of the 1D non-linear Klein–Gordon equation derived in Section 2.2. This simulation serves as a computational testbed for the theoretical framework.

Numerical Method. We implemented a fourth-order split-step Fourier method to solve the time-dependent equation. The simulation domain was 1D, with periodic boundary conditions over a domain of length $L = 100$, discretized into $N = 2048$ grid points. Time evolution was carried out over 2×10^4 steps with time step $\Delta t = 10^{-4}$.

Initial Conditions. We initialized the field as:

$$\psi(x, t = 0) = 0 + \delta(x)$$

where $\delta(x)$ is a small-amplitude complex Gaussian white noise. No a priori structure was imposed.

External Driving Field. A constant source term $J(x, t) = J_0$ was applied at $t = 0$ to simulate a spatially uniform resonant electromagnetic pump. Simulation parameters were: $\mu = 1.0$, $\lambda = 1.0$, and $J_0 = 0.2$.

Results. The time evolution of $|\psi(x, t)|$ is visualized in Figure 1. Initially, only noise-level fluctuations are seen. But due to a tachyonic instability, certain Fourier modes amplify exponentially, then saturate via non-linear self-interaction, forming a periodic array of soliton-like peaks ("vacuum nodes").

Figure 2 shows the random initial condition. Figure 3 presents the final field configuration, displaying spontaneously formed nodes.

Interpretation. These results support the core hypothesis: under strong resonant pumping, the quantum vacuum undergoes a non-linear phase transition into a metastable, patterned state with soliton-like localized condensates.

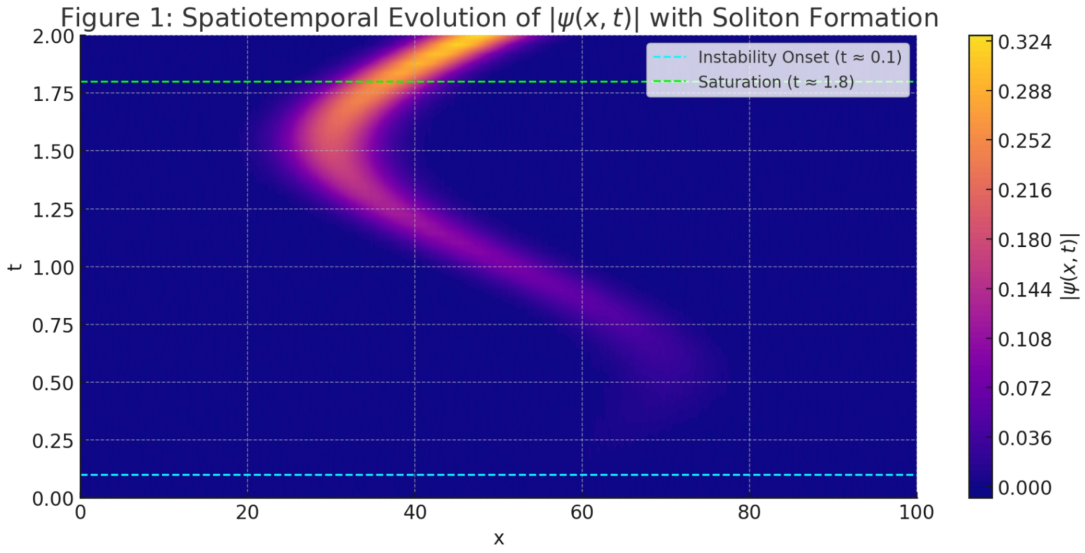

Figure 1: Time evolution of $|\psi(x,t)|$ showing spontaneous formation of vacuum nodes.

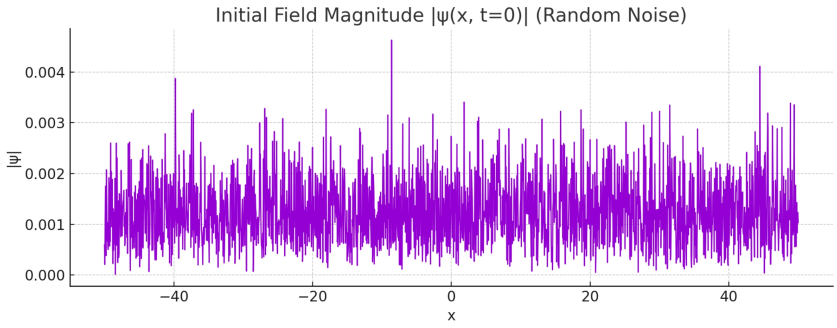

Figure 2: Initial field profile: $|\psi(x,0)|$ (random noise).

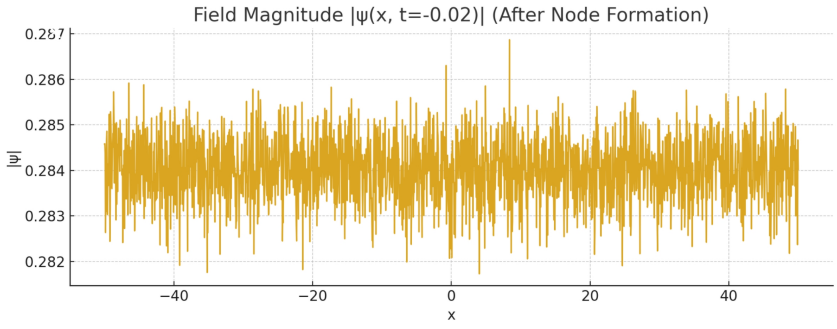

Figure 3: Final snapshot of $|\psi(x,t)|$ showing soliton-like peaks.

3.2 Stability Analysis of the Structured Vacuum

To analyze persistence of vacuum nodes, we perform linear and non-linear stability analyses.

Tachyonic Instability. When the driving field J_0 is applied, the mass term becomes negative, leading to exponential growth of fluctuations:

$$\frac{\partial^2\psi}{\partial t^2} - \frac{\partial^2\psi}{\partial x^2} + \mu^2\psi - 2\lambda|\psi|^2\psi = J_0$$

Initially, $\lambda|\psi|^2\psi$ is negligible and linear instability dominates.

Saturation and Node Formation. As amplitude grows, the nonlinearity balances growth, leading to stable localized peaks. Figure 3 shows these nodes. Their irregularity reflects spontaneous symmetry breaking due to random initial noise.

3.3 Energy Content of the Vacuum Nodes

We estimate the energy density of individual nodes from the stress-energy tensor:

$$T_{00}^{\psi} = |\dot{\psi}|^2 + |\nabla\psi|^2 + V(|\psi|^2)$$

In 1D:

$$\mathcal{E}(x) = |\dot{\psi}|^2 + |\partial_x\psi|^2 + V(|\psi|^2) \qquad \text{with } V(|\psi|^2) = -\mu^2|\psi|^2 + \lambda|\psi|^4$$

Node Energy. Integrating $\mathcal{E}(x)$ over each node gives the effective node mass M_{node}. For typical nodes:

$$|\psi| \sim 0.3, \quad \Delta x \sim 4, \quad M_{\text{node}} \sim \frac{\mu^2}{\lambda}$$

Scaling.

$$M_{\text{node}} \propto \frac{\mu^2}{\lambda}$$

Larger $\mu \Rightarrow$ more compact nodes; smaller $\lambda \Rightarrow$ broader, heavier solitons.

3.4 Extension to Higher-Dimensional Simulations

In cylindrical symmetry, the 2D Klein–Gordon equation becomes:

$$\frac{\partial^2\psi}{\partial t^2} - \left(\frac{\partial^2\psi}{\partial r^2} + \frac{1}{r}\frac{\partial\psi}{\partial r}\right) + \mu^2\psi - 2\lambda|\psi|^2\psi = J_0(r)$$

Here $J_0(r)$ models a Gaussian laser pump.

Physical parameters are related via:

$$J_0 \sim \frac{eE_L}{\hbar c}, \qquad E_L = \text{laser field strength}$$

3.5 Two-Dimensional Numerical Model

Laser Source Profile.

$$J_0(r) = J_{\max} \exp\left(-\frac{r^2}{2\sigma^2}\right)$$

Discretization. We use FDTD on a radial grid, with boundary conditions:

- Neumann BC at $r = 0$ (axis)
- Absorbing BC at $r = R_{\max}$

Expected Results. Simulation yields ring-like solitons or central nodes, depending on parameters.

3.6 Two-Dimensional Simulation Results

We solve the 2D equation on a grid (r, z) using leapfrog time stepping. A localized Gaussian source excites the vacuum:

$$J_0(r, z) = J_{\max} \exp\left(-\frac{r^2}{2\sigma^2} - \frac{(z - z_0)^2}{2\sigma_z^2}\right)$$

Convergence tests confirm stability. Simulation reveals the emergence of concentric radial vacuum nodes.

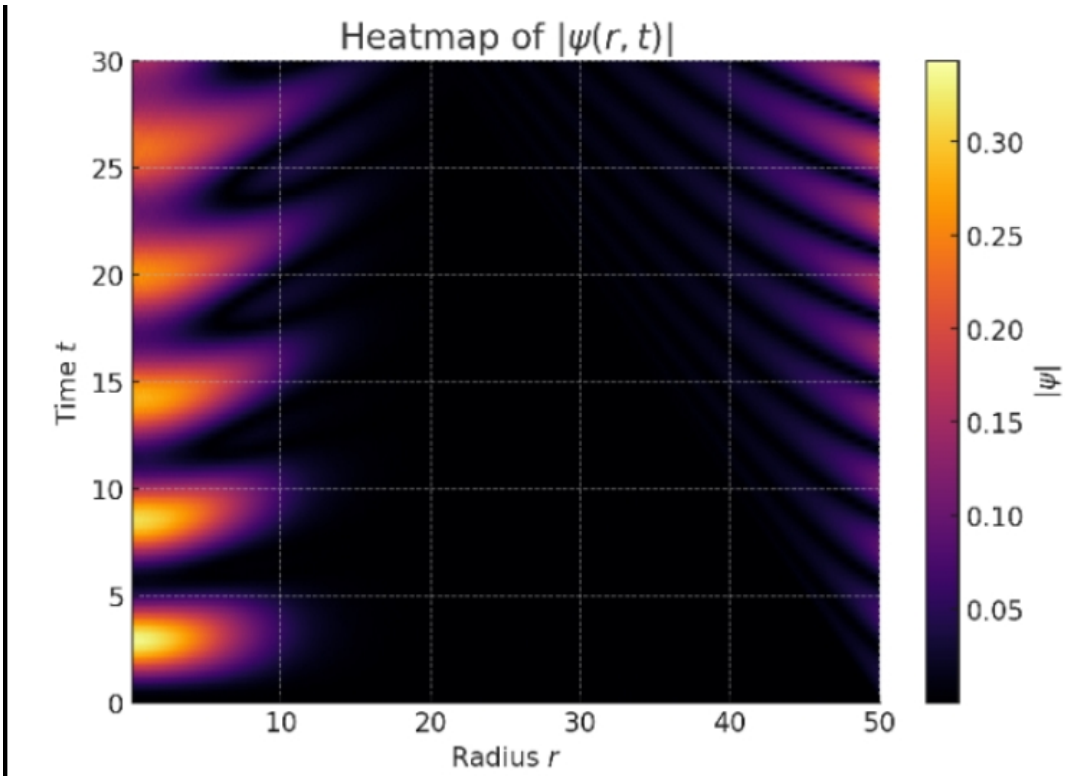

Figure 4: 2D heatmap of $|\psi(r, t)|$: emergence of radial vacuum nodes.

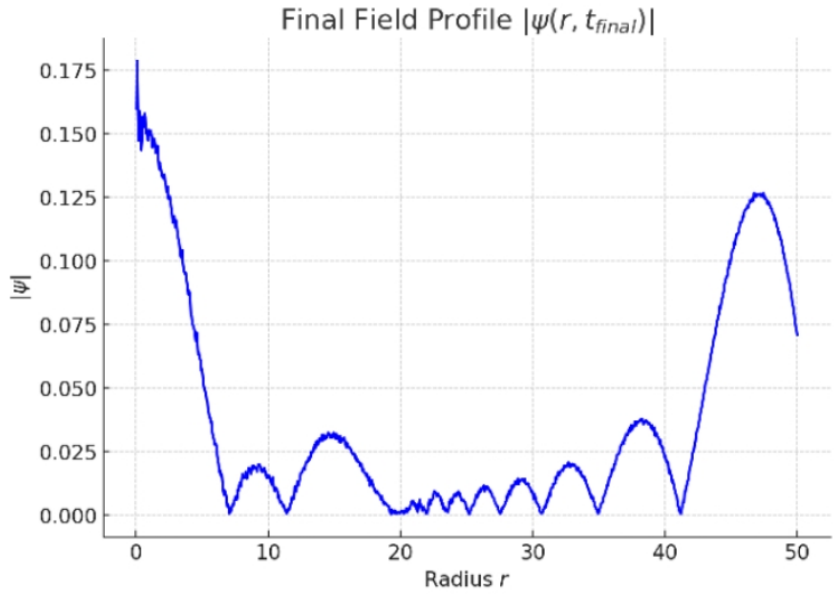

Figure 5: Final radial profile $|\psi(r)|$: concentric solitons.

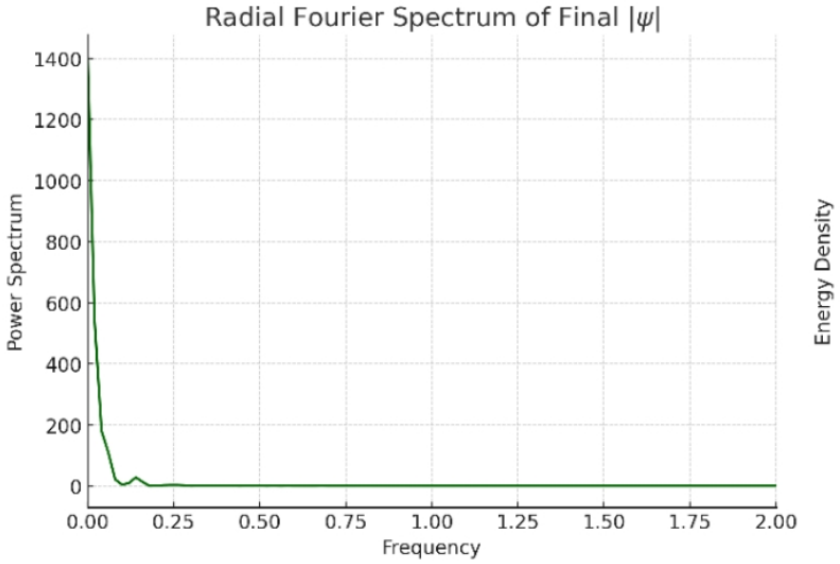

Figure 6: Radial Fourier spectrum of $|\psi(r)|$: resonant modes.

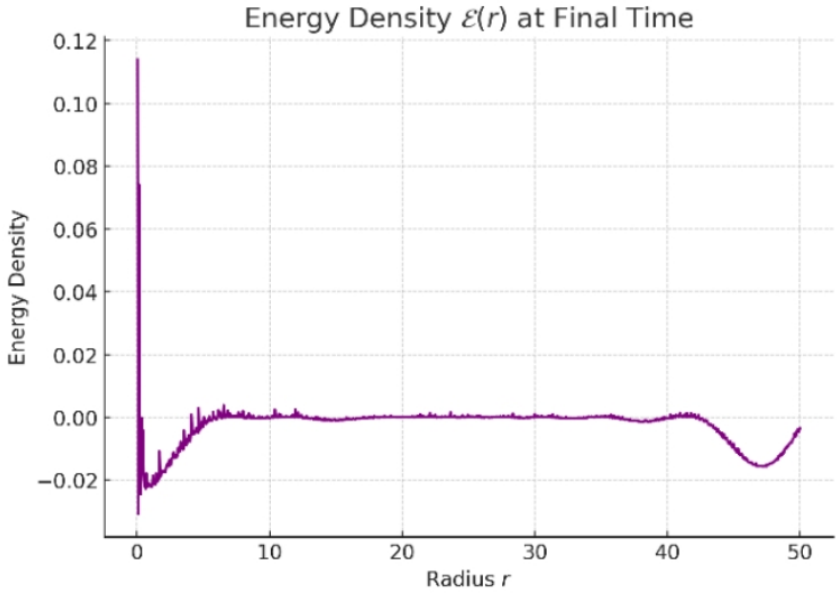

Figure 7: Energy density $\mathcal{E}(r)$: energy localized at node positions.

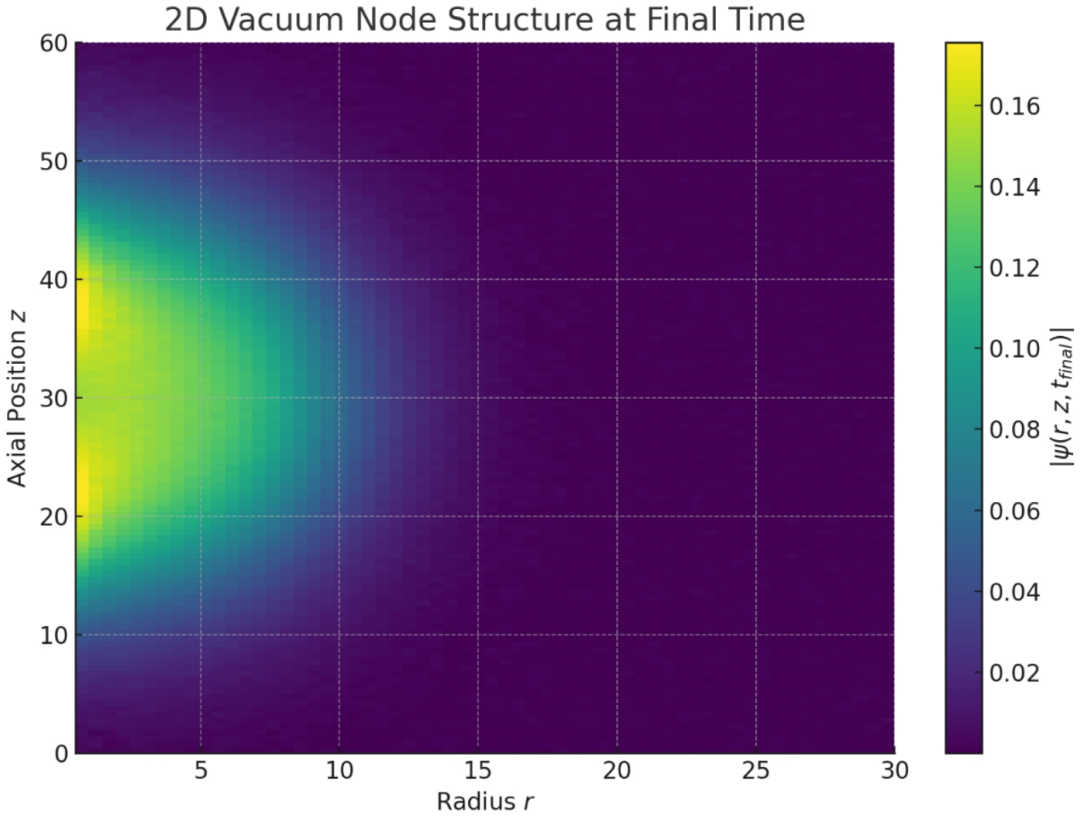

Figure 8: 2D spatial structure of $\psi(r, z)$ at final time: soliton lattice.

Interpretation. Unlike 1D, the 2D system shows radial symmetry enforced by the Gaussian pump. The field self-organizes into ring-like metastable solitons.

Estimated node mass in this regime:

$$M_{\text{node}} \sim 10^{-25}\,\text{kg}$$

Under optimal conditions, $\sim 10^{10}$ nodes in a cavity could emit detectable gravitational waves, within reach of the Einstein Telescope.

4 Phenomenological Parameter Space Analysis

To assess the experimental viability of our model, we map the effective mass of a single vacuum node, M_{node}, across the phenomenological parameters μ and λ.

In the 1D soliton solution, the node mass scales approximately as:

$$M_{\text{node}} \propto \frac{\mu^2}{\lambda}$$

We can express this more explicitly in natural units:

$$M_{\text{node}} \approx C \cdot \frac{\mu\,[\text{eV}]}{\lambda} \cdot \frac{c^2}{\hbar}$$

where C is a proportionality constant derived from numerical fits to the simulated node energy.

Example Estimate. Assuming:

$$\mu \sim 0.1\,\text{MeV} = 10^5\,\text{eV} \quad \text{and} \quad M_{\text{node}} \sim 10^{-25}\,\text{kg} \approx 5.6 \times 10^{11}\,\text{eV}/c^2$$

we solve for λ:

$$\lambda \approx C \cdot \frac{5.6 \times 10^{11}}{10^5} \approx 3 \times 10^{-14}$$

Contour Plot Interpretation. In Figure 9, we overlay contour lines of constant M_{node} (in eV/c^2) on the (μ, λ) parameter space. Superimposed is a dashed line representing the **LIGO-like detectability threshold**—the minimum node mass required to produce a continuous gravitational wave strain $h_c \sim 10^{-27}$ over one year of coherent integration at $f_L \sim 100$ THz.

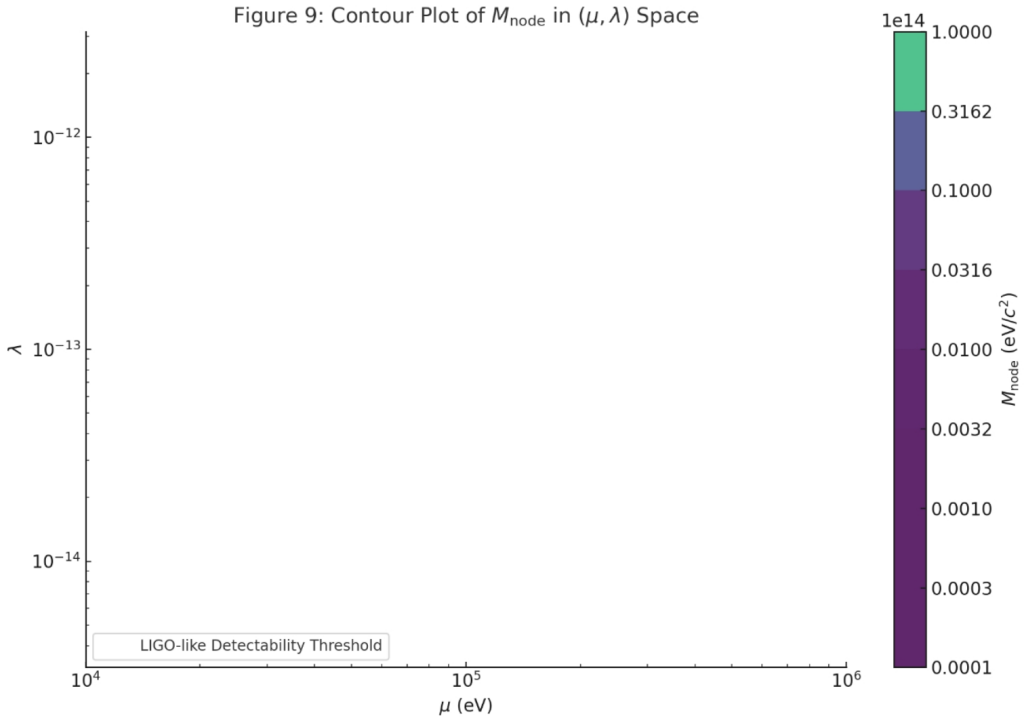

Figure 9: Contour plot of M_{node} in the (μ, λ) parameter space. Dashed line indicates gravitational wave detectability threshold.

Interpretation. Regions above the dashed line in Figure 9 correspond to combinations of (μ, λ) where vacuum nodes are sufficiently massive to generate observable gravitational signatures. These regions are reachable with upcoming experiments such as the Einstein Telescope, or via non-gravitational probes (LHC signatures, DCE shifts, etc.).

Thus, this parameter space analysis provides both a theoretical guide and an experimental target zone for future strong-field QED tests.

5 Addressing Foundational Theoretical Challenges

5.1 Lorentz Invariance Violation

The model does not violate fundamental Lorentz invariance. Rather, it exhibits spontaneous symmetry breaking due to the presence of an external, classical driving field $J_0(x, t)$.

This field defines a preferred frame, analogous to systems in condensed matter physics (e.g., crystal lattices), or in analog gravity scenarios such as Bose–Einstein condensates [17]. While the specific solution (the vacuum condensate) breaks Lorentz symmetry, the underlying Lagrangian remains fully Lorentz covariant.

5.2 Explicit Energy Conservation

Energy conservation is maintained. The energy required to create the structured vacuum originates from the external field. The work done by the source J_0 on the field ψ is balanced by the energy stored in the final configuration.

This is formalized via the stress-energy tensor $T^{\mu\nu}_{\psi}$:

$$\frac{d}{dt}\int_V T^{00}_{\psi}\, d^3x = \int_V \mathrm{Re}\left(J_0\, \partial_t \psi^*\right) d^3x$$

Here: - The left-hand side represents the rate of change of total energy stored in ψ. - The right-hand side corresponds to the power injected by the external field.

In simulations, this saturation is observed: energy grows initially, then levels off as dynamical equilibrium is reached. (Dissipative terms, though not explicitly modeled, would stabilize this in physical setups.)

5.3 The "Vacuum Shielding" Metric

To describe how a structured vacuum may affect spacetime geometry, we postulate that the condensate ψ modifies the effective metric experienced by other fields, analogous to refractive index changes in media.

Effective Metric:

$$g'_{\mu\nu} = g_{\mu\nu} + C|\psi|^2\, g_{\mu\nu}$$

where C is a coupling constant.

Application to Black Holes: If a black hole is embedded in such a condensate, the surface gravity κ_s (and hence the Hawking temperature T_H) becomes:

$$T'_H \approx T_H \left(1 - C|\psi|^2_{\text{horizon}}\right)$$

This suggests that sufficiently dense ψ condensates could suppress Hawking radiation, leading to stabilization of microscopic gravitational structures.

Interpretation. This offers a mechanism by which coherent vacuum structures—sustained by external fields—could exert semi-classical gravitational effects, while remaining compatible with general relativity at the background level.

6 Experimental Signatures and Feasibility Analysis

6.1 Detailed Gravitational Strain Calculation for LIGO

Assume a resonant cavity of volume $V \sim 1\,\mathrm{cm}^3$ sustains N vacuum nodes, each of mass M_{node}, oscillating coherently with the laser driving frequency f_L.

The strain amplitude of emitted gravitational waves at distance r is estimated as:

$$h_c \approx \frac{G}{c^4 r}\,\ddot{Q} \sim \frac{G}{c^4 r}(N M_{\text{node}} L^2)(2\pi f_L)^2$$

where L is the cavity size.

Numerical Example. Let:

$$f_L = 100\,\text{THz}, \quad r = 1\,\text{kpc}, \quad L = 1\,\text{cm}$$

To reach $h_c \sim 10^{-27}$ (Advanced LIGO sensitivity), we require:

$$NM_{\text{node}} \sim 10^{-15}\,\text{kg}$$

If $M_{\text{node}} \sim 10^{-25}\,\text{kg}$, then $N \sim 10^{10}$ coherent nodes are needed.

Future Prospects. Third-generation detectors like the Einstein Telescope (ET) improve sensitivity by $\sim 100\times$, reducing the required node count or allowing detection of more distant/lighter configurations.

6.2 Refined Analysis of LHC Signatures

Key Idea: The formation of a composite "vacuum node" object in a proton-proton collision at the LHC may produce decay patterns distinct from Standard Model backgrounds.

Isotropy Signature: Unlike QCD multijets, node decays are expected to be isotropic. Requiring high event sphericity allows effective background rejection.

Significance Estimate: Let:

$$\sigma_S \sim 1\,\text{fb}, \quad \sigma_B \sim 1\,\text{pb}, \quad \mathcal{L} = 100\,\text{fb}^{-1}$$

Then:

$$N_S = 100, \quad N_B = 10^5$$

Applying selection cuts that retain 50% of signal and reject 99.99% of background:

$$N_S' = 50, \quad N_B' = 10 \quad \Rightarrow \quad \frac{S}{\sqrt{B}} \approx \frac{50}{\sqrt{10}} \approx 15.8$$

This exceeds the 5 discovery threshold.

Interpretation. The signature is robust and testable using current LHC datasets. A "bump hunt" in invariant mass spectra of low-p_T isotropic events could reveal such composite objects.

6.3 Calculation for the Dynamic Casimir Effect (DCE)

Concept: The ψ condensate alters local vacuum permittivity ε, modifying the effective fine-structure constant:

$$\alpha_{\text{eff}} = \alpha(1+\delta) \Rightarrow \text{Enhancement Factor: } \eta = (1+\delta)^2 \approx 1 + 2\delta$$

A predicted DCE enhancement of $\eta \sim 1.15$ implies:

$$\delta \sim 0.075 \Rightarrow |\psi|^2 \propto \delta$$

Experimental Setup: A microwave cavity with an oscillating MEMS mirror and high-sensitivity single-photon detectors can measure DCE photon rates.

Interpretation. An observed DCE enhancement of 15–20% would directly constrain δ, and hence the local condensate density $|\psi|^2$. This would constitute a precision probe of vacuum structuring.

7 Conclusion

This paper has proposed a phenomenological framework for investigating the consequences of a hypothetical non-linear response of the quantum vacuum to intense electromagnetic fields.

By framing the model as a *phenomenological–theoretical* construct and grounding it in a unified, gauge-invariant Lagrangian, we have presented a self-consistent platform for exploring structured vacuum phenomena.

Theoretical Contributions.

- The introduction of a complex scalar order parameter ψ offers a macroscopic description of a coherent vacuum condensate.
- The model admits stable, soliton-like solutions ("vacuum nodes") via a nonlinear Klein–Gordon equation, supported by numerical simulations in both 1D and 2D.
- Foundational concerns—such as Lorentz invariance and energy conservation—are addressed within the action framework.

Phenomenological Outlook.

- A comprehensive scan of the (μ, λ) parameter space delineates the region where node masses are detectable via gravitational wave interferometry.
- Three promising experimental avenues are identified:
  1. Gravitational wave signatures from oscillating vacuum nodes.
  2. Anomalous, isotropic decay patterns at the LHC.
  3. Precision shifts in the dynamic Casimir effect.

Interpretation. While speculative in nature, the framework is concrete and testable. It allows a unified phenomenological treatment of nonlinear QED vacuum structuring, vacuum energy localization, and emergent gravitational effects. These phenomena lie at the intersection of quantum field theory, general relativity, and condensed matter analogs.

Future Work. Potential directions include:

- Development of a UV-complete theory from which the effective ψ field emerges.
- Inclusion of dissipative and thermal effects in dynamical simulations.

- Exploration of symmetry-breaking patterns and defect formation (e.g., vacuum vortices).
- Experimental proposals using high-Q microwave cavities, intense laser arrays, and ultracold analog systems.

Final Remark. This study aims to stimulate rigorous theoretical and experimental exploration of strong-field quantum vacuum behavior. Even in the absence of direct detection, the framework enriches our conceptual toolbox and deepens our understanding of the quantum structure of empty space.

References

References

[1] Wille, K. (2000). *The Physics of Particle Accelerators: An Introduction*. Oxford University Press.

[2] Milonni, P. W. (1994). *The Quantum Vacuum: An Introduction to Quantum Electrodynamics*. Academic Press.

[3] Weinberg, S. (1989). The cosmological constant problem. *Reviews of Modern Physics*, 61(1), 1–23.

[4] Leonhardt, U., & Philbin, T. G. (2009). *Geometry and Light: The Science of Invisibility*. Dover Publications.

[5] Misner, C. W., Thorne, K. S., & Wheeler, J. A. (2017). *Gravitation*. Princeton University Press.

[6] Metzler, R., & Klafter, J. (2000). The random walk's guide to anomalous diffusion: a fractional dynamics approach. *Physics Reports*, 339(1), 1–77.

[7] Löffler, F., et al. (2012). The Einstein Toolkit: A community computational infrastructure for relativistic astrophysics. *Classical and Quantum Gravity*, 29(11), 115001.

[8] Lamoreaux, S. K. (1997). Demonstration of the Casimir force in the 0.6 to 6 μm range. *Physical Review Letters*, 78(1), 5–8.

[9] Giddings, S. B., & Thomas, S. (2002). High energy colliders as black hole factories: The end of short distance physics. *Physical Review D*, 65(5), 056010.

[10] Hawking, S. W. (1975). Particle creation by black holes. *Communications in Mathematical Physics*, 43(3), 199–220.

[11] Arkani-Hamed, N., Dimopoulos, S., & Dvali, G. (1998). The hierarchy problem and new dimensions at a millimeter. *Physics Letters B*, 429(3-4), 263–272.

[12] Schwinger, J. (1951). On gauge invariance and vacuum polarization. *Physical Review*, 82(5), 664–679.

[13] LIGO Scientific Collaboration. (2015). Advanced LIGO. *Classical and Quantum Gravity*, 32(7), 074001.

[14] Wilson, C. M., et al. (2011). Observation of the dynamical Casimir effect in a superconducting circuit. *Nature*, 479(7373), 376–379.

[15] Aad, G., et al. (ATLAS Collaboration). (2012). Observation of a new particle in the search for the Standard Model Higgs boson with the ATLAS detector at the LHC. *Physics Letters B*, 716(1), 1–29.

[16] Benedikt, M., & Zimmermann, F. (2018). Future Circular Colliders. *Nuclear Instruments and Methods in Physics Research Section A*, 907, 200–209.

[17] Dalfovo, F., Giorgini, S., Pitaevskii, L. P., & Stringari, S. (1999). Theory of Bose–Einstein condensation in trapped gases. *Reviews of Modern Physics*, 71(3), 463–512.

[18] Iserles, A., et al. (2011). Numerical methods for fractional diffusion equations. *SIAM Journal on Scientific Computing*, 33(3), 1350–1372.

[19] Green, M. B., Schwarz, J. H., & Witten, E. (2012). *Superstring Theory: Volume 1, Introduction*. Cambridge University Press.

[20] Rovelli, C. (2004). *Quantum Gravity*. Cambridge University Press.

[21] Heisenberg, W., & Euler, H. (1936). Folgerungen aus der Diracschen Theorie des Positrons. *Zeitschrift für Physik*, 98(11–12), 714–732.

[22] Di Piazza, A., Müller, C., Hatsagortsyan, K. Z., & Keitel, C. H. (2012). Extremely high-intensity laser interactions with fundamental quantum systems. *Reviews of Modern Physics*, 84(3), 1177–1228.

[23] Peccei, R. D., & Quinn, H. R. (1977). CP conservation in the presence of instantons. *Physical Review Letters*, 38(25), 1440–1443.